

*Present address: Deutsches Elektronen Synchrotron, Notkestieg 1, 2000 Hamburg-52, Germany.

†Work supported by the Swiss Institute for Nuclear Research (S. I. N.).

‡Research work supported in part by the Atomic Energy Control Board of Canada.

¹The preliminary results of this experiment have been presented by J. C. Alder, W. Kossler, C. F. Perdrisat, W. K. Roberts, P. Kitching, G. Moss, W. C. Olsen, and J. R. Priest, *Bull. Am. Phys. Soc.* **16**, 132 (1971).

²A value of $(d\sigma/d\Omega)_{pd} = 0.050 \pm 0.002$ mb/sr was used; see J. S. Vincent, W. K. Roberts, E. T. Boschitz, L. S.

Kisslinger, K. Gotow, P. C. Gugelot, C. F. Perdrisat, L. W. Swenson, and J. R. Priest, *Phys. Rev. Letters* **24**, 236 (1970).

³H. Davies, H. Muirhead, and J. N. Wouds, *Nucl. Phys.* **78**, 663 (1966).

⁴Yu. A. Kudeyarov, I. V. Kurdyumov, V. G. Neudatchin, and Yu. F. Smirnov, *Nucl. Phys.* **A163**, 316 (1971).

⁵I. V. Kurdyumov, Ph.D. thesis, Nuclear Research Institute, Moscow State University, 1971 (unpublished); and private communication with V. G. Neudatchin.

⁶Y. C. Tang, K. Wildermuth, and L. D. Pearlstein, *Phys. Rev.* **123**, 548 (1961).

PHYSICAL REVIEW C

VOLUME 6, NUMBER 1

JULY 1972

${}^{19}\text{F}(d, p){}^{20}\text{F}$ and the Nuclear Structure of ${}^{20}\text{F}^\dagger$

H. T. Fortune*

*Argonne National Laboratory, Argonne, Illinois 60439,
and Physics Department, University of Pennsylvania, Philadelphia, Pennsylvania 19104*

and

G. C. Morrison, R. C. Bearse,‡ and J. L. Yntema

Argonne National Laboratory, Argonne, Illinois 60439

and

B. H. Wildenthal

Physics Department, Michigan State University, East Lansing, Michigan 48823

(Received 6 December 1971)

The reaction ${}^{19}\text{F}(d, p){}^{20}\text{F}$ has been studied with 16-MeV deuterons. Outgoing protons were detected in photographic emulsions in a magnetic spectrograph. Spectroscopic factors were extracted and combined with previous information and compared with results of shell-model calculations performed in a complete sd -shell basis. Of the previously known 25 states below $E_x = 4.5$ MeV, angular distributions measured at 14 angles were obtained for all but the 5 at $E_x = 1.824, 2.871, 3.761, 4.20,$ and 4.21 MeV. Strong stripping angular distributions were observed for 10 states—6 dominated by $l = 2$, and 4 by $l = 0$. These 10 states agree reasonably well in position and strength with the 10 lowest shell-model states predicted to have appreciable amounts of the configuration [${}^{19}\text{F}(\text{g.s.}) \otimes 1d_{5/2}$ or $2s_{1/2}$ neutron].

I. INTRODUCTION

The spectroscopy of ${}^{20}\text{F}$ is typical of non-self-conjugate odd-odd nuclei; the knowledge about it is extremely scant in view of the effort that has been expended. The most notable early work on its structure was that of El Bedewi¹ in 1956. Using an 8.9-MeV deuteron beam and one of the first heavy-particle spectrographs, he was able to obtain excitation energies and angular distributions for a great many of the states in ${}^{20}\text{F}$. His analysis of the angular distributions was limited by the use of the plane-wave Born approximation (PWBA). However, as we shall see below, his results for the few strong states were qualitatively correct.

Accurate excitation energies have been mea-

sured² up to $E_x = 6.043$ MeV by use of the reactions ${}^{18}\text{O}({}^3\text{He}, p){}^{20}\text{F}$ and ${}^{19}\text{F}(d, p){}^{20}\text{F}$ at low bombarding energies. Information on the γ decay of levels of ${}^{20}\text{F}$ has been obtained in studies of the reactions ${}^{18}\text{O}({}^3\text{He}, p\gamma){}^{20}\text{F}$,³⁻⁷ ${}^{19}\text{F}(d, p\gamma){}^{20}\text{F}$,^{3,8} ${}^{19}\text{F}(n, \gamma){}^{20}\text{F}$,⁹⁻¹² and ${}^{18}\text{O}(t, n\gamma){}^{20}\text{F}$.¹³ Further studies include measurements of lifetimes¹³⁻¹⁶ of excited ${}^{20}\text{F}$ levels, angular-distribution measurements of the reaction ${}^{19}\text{F}(d, p){}^{20}\text{F}$ obtained with a polarized deuteron beam,¹⁷ and a study of the reaction ${}^{22}\text{Ne}(p, {}^3\text{He})-{}^{20}\text{F}$.¹⁸ Studies of the reactions ${}^{18}\text{O}({}^3\text{He}, p){}^{20}\text{F}$ and ${}^{22}\text{Ne}(d, \alpha){}^{20}\text{F}$ have also been reported recently.¹⁹ The experimental results concerning ${}^{20}\text{F}$ are excellently summarized in the review by Ajzenberg-Selove.²⁰

Directional-correlation measurements⁷ in the re-

action $^{18}\text{O}(^3\text{He}, p\gamma)^{20}\text{F}$ led to limits on the spins of most states below 3 MeV in excitation. The new spin assignments were considered unambiguous for only two states: 3^+ for the state at 0.656 MeV and 2^+ for the 2.044-MeV state. Unique spin assignments for the other states are difficult to determine in such correlation experiments because of the relatively high spin of the ground state of ^{20}F , for which $J^\pi = 2^+$.²¹ The 1.06-MeV state has been known for some time to have $J^\pi = 1^+$.²² Other spin-parity assignments made concurrently with the present work will be discussed further below.

There has not been extensive theoretical study of the level structure of ^{20}F , in part because of the lack of definite experimental information and in part because the nucleus does not appear to be amenable to description in terms of the popular (simplest) nuclear models. Recently, calculations for all of the *sd*-shell nuclei with $A \leq 22$ have been carried out at Oak Ridge.²³ The results obtained for nuclear properties (energies, single-nucleon spectroscopic factors, and electromagnetic transition rates) have been in good enough agreement with existing experimental information in this region to suggest that an attempt to interpret the experimental data to be reported here in terms of these new theoretical results might be of significant help in understanding this rather complex nuclear system.

Single-nucleon-transfer spectroscopic factors yield rather specific information about the wave functions of nuclear states, and hence the comparison of theoretical and experimental *S* factors is a very important test of the predictions from nuclear models. At the same time, the model results can often illuminate the experimental picture. If a strong stripping state can be identified with a model state that is expected to be strong, a tentative "assignment" can be made, and this can then be used to find consistencies between the remaining states and the model.

Since the nuclear model used here is based on the complete *sd* shell with *1p*-shell hole states and *fp* particle states ignored, only states of positive parity will be predicted. Furthermore, spectroscopic factors can be predicted only for $s_{1/2}$, $d_{3/2}$, and $d_{5/2}$ transfer; all other transfer strengths are predicted as identically zero.

Only two targets are available for single-particle-transfer reactions to ^{20}F : ^{19}F may be used as a stripping target, ^{21}Ne as a pickup target. Using ^{21}Ne as a target poses some experimental difficulties, since it is available only as a gas and the abundance of ^{21}Ne in natural neon is only 0.26%. Since ^{21}Ne has a ground-state spin of $\frac{3}{2}^+$, there will be ambiguities in determining the spins of the residual states from the orbital angular momen-

tum transfer. Reactions on ^{19}F ($J^\pi = \frac{1}{2}^+$) are obviously easier to interpret; and it is easy to make targets of ^{19}F compounds. The reaction $^{19}\text{F}(d, p)^{20}\text{F}$ with $Q = 4.373$ MeV remains the most logical choice for a study of the single-particle strengths of the states of ^{20}F . Since the data of El Bedewi¹ were taken at an energy at which the direct reaction may not be dominant, we decided to look again at the reaction $^{19}\text{F}(d, p)^{20}\text{F}$ with 16-MeV deuterons from the Argonne tandem Van de Graaff accelerator. At this energy, direct processes should dominate, so that states having large cross sections are expected to be populated mainly via direct stripping. This was not the case at the lower energy, where the analysis of the data was complicated by the presence of nondirect mechanisms.

II. EXPERIMENTAL

Since it is known²⁰ that ^{20}F has at least 13 states below 3 MeV excitation and that several of these are less than 100 keV apart, it becomes important to choose a fluorine compound that will not contribute many additional lines to the already dense spectrum. Of the compounds normally used to make fluorine targets, LiF appeared to be the best for our purposes. The difference between $Q = -0.192$ MeV for the reaction $^7\text{Li}(d, p)^8\text{Li}$ and $Q = +4.373$ MeV for the reaction $^{19}\text{F}(d, p)^{20}\text{F}$ assures at least 4.5 MeV of excitation without interference from the other major constituent of the target. Unfortunately, Q is $+5.027$ MeV for $^6\text{Li}(d, p)^7\text{Li}$, so lines from this reaction are a possible source of interference. Fortunately, the ^6Li concentration in Li is only 7.4% and, further, ^7Li has only three final states below 6 MeV to be populated by the reaction. The results obtained here apparently indicate that the LiF used had been depleted in ^6Li , since no lines attributable to $^6\text{Li}(d, p)$ appear in the spectrum (Fig. 1). The LiF target was evaporated onto a supporting layer of C about $10 \mu\text{g}/\text{cm}^2$ thick.

The LiF targets deteriorated somewhat under bombardment, so it was necessary to continuously monitor the thickness. This was done by using a surface-barrier detector to count deuterons elastically scattered at 45° to the incident beam. The (*d, p*) results were normalized to the monitor counting rate at each angle.

To obtain absolute cross sections, we prepared a target of CaF_2 on a carbon backing and exposed it to a 12-MeV deuteron beam under the conditions described below for obtaining the (*d, p*) data. The elastic scattering counting rate from calcium at 95° , 100° , and 105° was determined and compared with the values of $d\sigma/d\Omega$ given by Bassel *et*

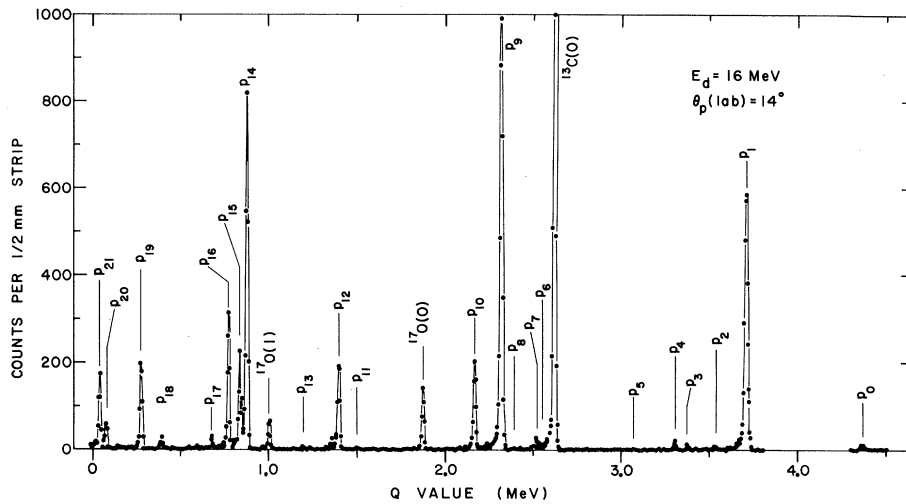


FIG. 1. Spectrum of protons from the reaction $^{19}\text{F}(d, p)^{20}\text{F}$, obtained at a deuteron energy of 16.0 MeV and a laboratory angle of 14° with a LiF target. Excitation energies are listed in Table I.

TABLE I. Excitation energies (MeV \pm keV) in ^{20}F .

Group number ^a	Present work ^b	Literature (Ref. 19)
0	0	0
1	0.655 \pm 1	0.655 95 \pm 0.15
2	0.823 \pm 5	0.8229 \pm 0.2
3	0.983 \pm 5	0.9838 \pm 0.2
4	1.056 \pm 3	1.056 93 \pm 0.16
5	1.309 \pm 5	1.309 22 \pm 0.16
6	1.82 \pm 10 ^c	1.8244 \pm 1.3
7	1.845 \pm 4	1.8434 \pm 0.3
8	1.97 \pm 10 ^c	1.9706 \pm 0.3
9	2.044 \pm 1	2.0439 \pm 0.3
10	2.196 \pm 1	2.1946 \pm 0.5
11	2.871 \pm 5	2.865 \pm 1.5
12	2.966 \pm 1	2.9662 \pm 0.4
13	3.176 \pm 5	3.1746 \pm 1.2
14	3.489 \pm 1	3.4884 \pm 0.2
15	3.531 \pm 3	3.5259 \pm 0.4
16	3.590 \pm 1	3.5871 \pm 0.3
17	3.686 \pm 4	3.6810 \pm 0.4
	d	3.761 \pm 2
18	3.977 \pm 5	3.9662 \pm 1.4
19	4.089 \pm 3	4.0824 \pm 0.4
	d	4.1989 \pm 2.7
	d	4.2077 \pm 2.6
20	4.282 \pm 5	4.2766 \pm 0.5
21	4.318 \pm 5	4.3115 \pm 2.6

^a Group numbers correspond to the labeling in Fig. 1.

^b Obtained by averaging the excitation energies obtained at the 14 angles at which measurements were taken.

^c Not observed at a sufficient number of angles to obtain accurate excitation energies.

^d Not observed in the present experiment.

*al.*²⁴ The same target was then used at 16 MeV to obtain a $^{19}\text{F}(d, p)^{20}\text{F}$ spectrum at $\theta_{\text{lab}} = 14^\circ$. On the assumption that there were two fluorine atoms for each calcium atom, the differential cross section for the first excited state of ^{20}F at $\theta_{\text{lab}} = 14^\circ$ was determined to be $d\sigma/d\Omega = 5.5 \pm 0.5$ mb/sr. All the other data points were then normalized to this value.

Data on the $^{19}\text{F}(d, p)$ reaction for 16-MeV deuterons were taken at 14 angles between 8 and 44° (lab) with the Argonne Browne-Buechner spectrograph. The particles were detected with NTB-50 emulsions. To increase the sensitivity of these emulsions to high-energy protons, they were covered with 30-mil acetate foil to degrade the incident proton energy. This increased the stopping power for protons and increased the track brightness.

The plates were scanned by hand in 0.5-mm strips from the position of the ground state to the position of the 4.32-MeV excited state in ^{20}F at each angle. The results for $\theta_{\text{lab}} = 14^\circ$ are shown in Fig. 1. Excitation energies for 21 excited states below 4.5 MeV were obtained at each angle. The averaged results are shown in Table I, along with the values from the literature.²⁰ Angular distributions are exhibited in Figs. 2 and 3.

III. ANALYSIS

The experimental angular distributions were compared with distorted-wave Born-approximation (DWBA) calculations with the code DWUCK²⁵

by use of the relation

$$\sigma_{\text{exp}}(\theta) = N \frac{2J_f + 1}{2J_i + 1} \sum_{i,j} \frac{S_{ij} \sigma_{ij}(\theta)}{2j + 1}.$$

For a (d, p) reaction, the normalization factor is conventionally taken to be $N = 1.65$.

The bound-state form factor for the transferred neutron was taken to be the wave function of a neutron in a Woods-Saxon well, with a binding energy equal to the difference between the ground-state separation energy and the excitation energy of the state in ^{20}F . The bound-state parameters are listed in Table II. The optical-model parameters used in the DWBA calculations were taken from earlier work in this mass region.^{26,27} The optical-model parameters for the exit channel were obtained by extrapolation from the average parameters of Watson, Singh, and Segel,²⁷ who systematically analyzed proton elastic scattering data from a number of light nuclei. Their parameters are given as a function of target mass and bombarding energy for target nuclei in the $1p$ shell, but are still expected to be a reasonable representation for a nucleus as light as ^{20}F . These pa-

rameters for ^{20}F are listed in Table II for the proton energy corresponding to the ground-state transition at a deuteron energy of 16 MeV. Since the calculations proved to be relatively insensitive to small changes in these parameters, this proton potential was used for all final states observed in the present experiment.

For the entrance channel, deuteron optical-model parameters corresponding to a bombarding energy of 16 MeV are not available. Hence, calculations were performed for a large number of different sets of deuteron optical-model potentials. Even though several potential sets gave satisfactory fits to the (d, p) angular distributions, none of them was successful in reproducing the $l=2$ shape observed at extreme forward angles. Furthermore, *absolute* spectroscopic factors extracted with the different potentials differed by as much as 50%. Similar variations were noted for the ratio of $l=0$ to $l=2$ spectroscopic factors. For fixed l value, however, the relative spectroscopic factors were virtually independent of the potential used. The deuteron potential chosen for the final calculations is listed in Table II. This potential has been used for several reactions involving deuterons and nu-

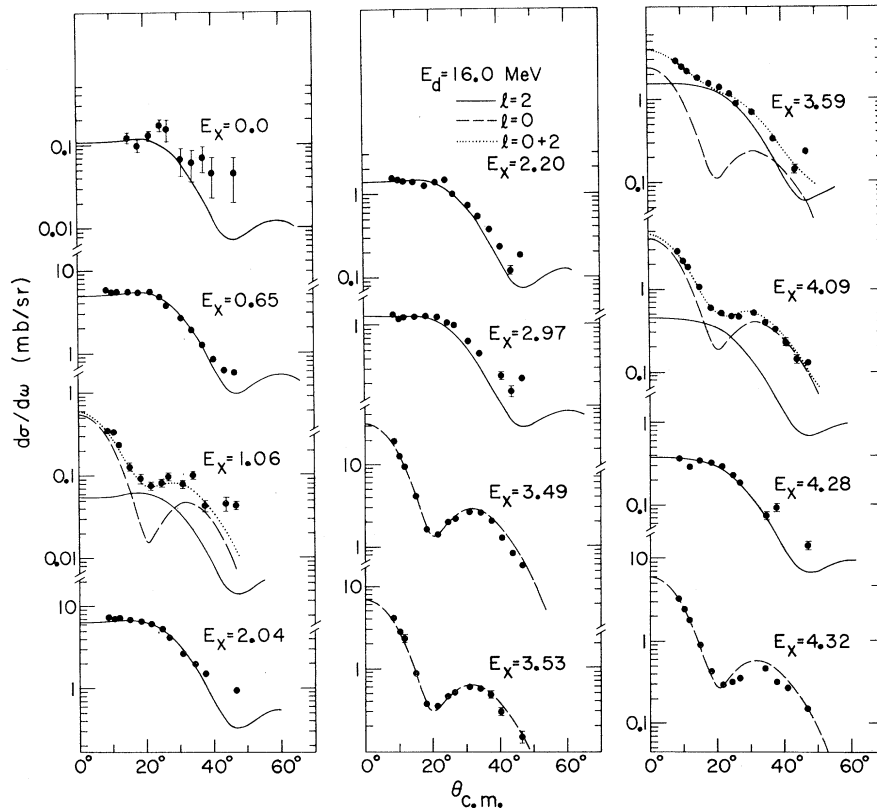


FIG. 2. Angular distributions of the reaction $^{19}\text{F}(d, p)^{20}\text{F}$ for strong states below 4.5 MeV and for states having obvious shell-model counterparts. The curves are the results of DWBA calculations as described in the text.

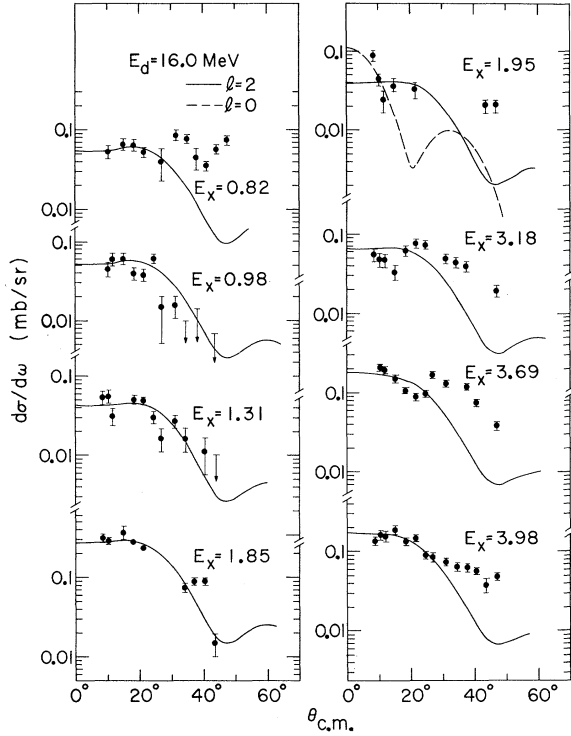


FIG. 3. Angular distributions of the reaction $^{19}\text{F}(d, p)^{20}\text{F}$ for weak states and/or states not possessing an obvious shell-model counterpart. In general, as explained in the text, these data are insufficient to allow l -value assignments to be made.

clei in the sd shell.²⁶ For the final calculations, finite-range nonlocal (FRNL) corrections were applied.

The results of DWBA calculations for all the states observed in the present work are plotted in Figs. 2 and 3, along with the data. Spectroscopic strengths were extracted and are listed in Table III. For the extremely weak states, the values of n , l , and j are in parentheses. For these states, the l values should not be taken as assignments, the values of $(2J+1)S$ merely reflect the weakness of the cross section, and the value of J^π need not be consistent with the listed l . Placing the value of $(2J+1)S$ also in parentheses indicates that the

presence of the l value listed in the middle column has not been established—usually because some other l is dominant in the angular distributions.

Since $^{19}\text{F}(\text{g.s.})$ has $J^\pi = \frac{1}{2}^+$, the observation of $l=2$ in the reaction $^{19}\text{F}(d, p)^{20}\text{F}$ limits the spin to $J=1-3$ with positive parity. An $l=0$ angular distribution implies positive parity and $J=0$ or 1. Combining these two, we see that an admixed $l=0+2$ angular distribution is possible only if the final state has $J^\pi = 1^+$. Therefore, the present results (Fig. 2) imply $J^\pi = 1^+$ for the 4.089-MeV state, and $J^\pi = 0^+$ or 1^+ for the 3.489-, 3.531-, and 4.318-MeV states. The 3.489-MeV state has recently been assigned¹⁹ $J^\pi = 1^+$ and the 3.531-MeV state $J^\pi = 0^+$. The observed angular distribution for the 1.056-MeV state is consistent with its known $J^\pi = 1^+$.

The ground state of ^{20}F has $J^\pi = 2^+$, but the cross section for the reaction to this state is extremely small. States at $E_x = 0.655, 2.044, 2.196, 2.966,$ and 4.282 MeV appear to have angular distributions that are unambiguously characteristic of $l=2$. Thus, for these states $J^\pi = 1^+, 2^+,$ or 3^+ . These results are consistent with earlier assignments of 3^+ for the 0.655-MeV state and 2^+ for the 2.044-MeV state.

Because of the relatively poor fit to $l=2$ angular distributions at extreme forward angles, the evidence for an $l=0$ component in the angular distribution of the 3.590-MeV state is not sufficient to allow an assignment of 1^+ .

Angular distributions for the weak states are shown in Fig. 3. None of these are unambiguously characteristic of a definite l value, even though the 1.85-MeV state does appear to be reasonably well fitted by $l=2$. Earlier assignments¹ of $l=2$ in the reaction $^{19}\text{F}(d, p)^{20}\text{F}$ to states at $E_x = 0.83$ and 0.98 MeV are not substantiated by the present results. Thus the earlier J^π limits¹ of $1^+, 2^+, 3^+$ for these two states no longer hold insofar as they arose from the $l=2$ assignments¹ in the (d, p) reaction. Furthermore, the previous assignments¹ of $l=3$ for the 2.87-MeV state and $l=1$ for the 2.97-MeV state are not supported by the present data. El Bedewi's assignment¹ of $l=2$ for levels

TABLE II. Optical-model parameters used in the DWBA analysis of the reaction $^{19}\text{F}(d, p)^{20}\text{F}$ at $E_d = 16.0$ MeV.

Channel	V_0 (MeV)	$r_0 = r_{so}$ (F)	$a = a_{so}$ (F)	W (MeV)	$W' = 4W_D$ (MeV)	r'_0 (F)	a' (F)	V_{so} (MeV)	r_C (F)
$^{19}\text{F} + d$ ^a	105	1.02	0.86	0	80	1.42	0.65	6.0	1.30
$^{20}\text{F} + p$ ^b	57.07	1.144	0.57	0	33.92	1.144	0.50	5.5	1.144
Bound state	...	1.26	0.60	$\lambda = 25$...

^a Reference 26.

^b Reference 27.

at 0.65, 2.04, and 2.20 MeV, and of $l=0$ for levels at 1.06, 3.49, 4.08, and 4.31 MeV are consistent with our results. These states are discussed further below.

IV. DISCUSSION

The results of the present experiment are displayed in the first two columns of Fig. 4. The third column displays the ^{20}F energy levels predicted by a recent shell-model calculation, and the fourth column indicates the spectroscopic factors for the reaction $^{19}\text{F}(d, p)^{20}\text{F}$ as calculated from these shell-model wave functions.²³ The relationships between the experimental data and the theoretical predictions will be discussed in the following paragraphs.

The shell-model calculations for the levels of ^{20}F are obtained from a comprehensive study of nuclei with $18 \leq A \leq 22$. The basis space of the model spans the complete set of $(1d_{5/2})(2s_{1/2})(1d_{3/2})$ configurations. A closed $(1s_{1/2})(1p_{3/2})(1p_{1/2})$ core is assumed for ^{16}O . The model Hamiltonian is

TABLE III. Experimental spectroscopic strengths observed in the reaction $^{19}\text{F}(d, p)^{20}\text{F}$ at $E_d = 16.0$ MeV.

E_x (MeV)	nlj (Ref. a)	$(2J+1)S$
0.0	$(1d_{5/2})$	$\lesssim 0.06$
0.655	$1d_{5/2}$	2.59
0.823	$(1d_{5/2})$	$\lesssim 0.03$
1.056	$2s_{1/2}$	0.019
	$(1d_{3/2})$	$\lesssim 0.03$
1.309	$(1d_{5/2})$	$\lesssim 0.02$
1.824	$(1d_{5/2})$	$\lesssim 0.11$
1.840		
1.971	$(2s_{1/2})$	$\lesssim 0.004$
	$(1d_{3/2})$	$\lesssim 0.02$
2.044	$1d_{5/2}$	2.32
2.196	$1d_{5/2}$	0.50
2.871	$(1d_{5/2})$	$\lesssim 0.02$
2.966	$1d_{5/2}$	0.36
3.176	$(1d_{5/2})$	$\lesssim 0.02$
3.489	$2s_{1/2}$	1.20
3.531	$2s_{1/2}$	0.29
3.590	$(2s_{1/2})^b$	$(\lesssim 0.09)^b$
	$(1d_{3/2})$	0.42
3.686	$(1d_{5/2})$	$\lesssim 0.04$
3.977	$(1d_{5/2})$	$\lesssim 0.04$
4.089	$2s_{1/2}$	0.18
	$(1d_{3/2})^b$	$(0.10)^b$
4.282	$1d_{5/2}$	0.07
4.318	$2s_{1/2}$	0.27

^a An nlj value in parentheses is not an assignment, but merely represents the nlj value for which the DWBA curves in Figs. 2 and 3 were calculated.

^b At the sensitivity of the present experiment, this l value may not be present.

based on the work of Kuo.²⁸ In the initial calculations for this region, the 63 two-body matrix elements of the effective interaction were taken from Ref. 28 and the three single-particle energies were taken from the single-particle level scheme of ^{17}O . The results of this calculation are in generally good agreement with experimental energy-level information, but there is some evidence that empirical adjustment of some of the features of the Hamiltonian would improve agreement between experiment and theory. To make this adjustment, nine of the two-body matrix elements between two-particle states involving the $1d_{5/2}$ and $2s_{1/2}$ orbits and the three single-particle energies were varied so as to produce an rms minimum between the energies of 41 selected levels in the region and the corresponding shell-model eigenvalues. This procedure made use of the Coulomb-reduced binding energy of the ground state, but not of any other information about the ^{20}F levels. With this empirical modification of the Kuo interaction, the predictions for ^{20}F are presented in Fig. 4. (This calculation is designated $K+12$ FP in Ref. 23.) These results are quite similar to those for the unmodified interactions and generally resemble the results obtained with completely different parameterizations²³ of the $(1d_{5/2})(2s_{1/2})(1d_{3/2})$ Hamiltonian. Hence, many of the qualitative features of the theoretical results which we shall emphasize in the ensuing discussion can be considered to be standard features of the model space itself rather than

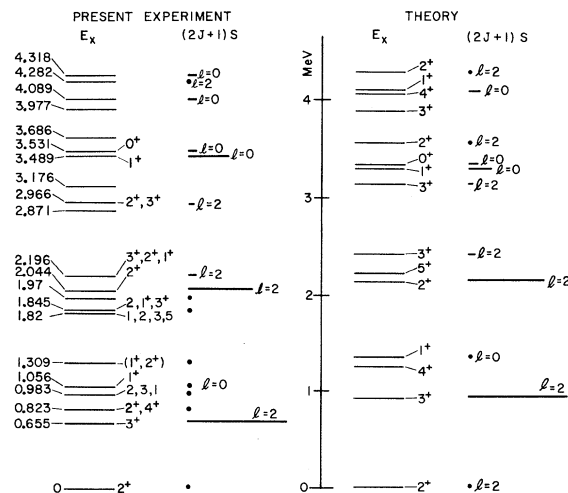


FIG. 4. Comparison of experimental (present work) and theoretical (Ref. 22) excitation energies and spectroscopic strengths in $^{19}\text{F}(d, p)^{20}\text{F}$. The experimental J^π values are from the literature *prior to the present work*. Dots represent spectroscopic strengths less than 0.15.

functions of the particular form of the effective Hamiltonian.

The ground state of the theoretical ^{20}F level scheme is 2^+ , in agreement with the experimental assignment for the ground state. Using the notation $(l_j)^n_{JT}$, the theoretical wave function for this state has probabilities of $\sim 40\%$ for $(d_{5/2})^4_{2,1}$, 10% for $(d_{5/2})^3_{3/2,3/2}(s_{1/2})^1$, and $\sim 5\%$ for $(d_{5/2})^3_{5/2,3/2}(s_{1/2})^1$. The model wave function for the $J^\pi = \frac{1}{2}^+$, $T = \frac{1}{2}$ ground state of ^{19}F contains such components as $(s_{1/2})^3$ with a probability of $\sim 10\%$, $(d_{5/2})^1(s_{1/2})^1(d_{3/2})^1$ with $\sim 10\%$, $(d_{5/2})^2_{1,0}(s_{1/2})^1$ with $\sim 10\%$, $(d_{5/2})^2_{0,1}(s_{1/2})^1$ with $\sim 30\%$, and $(d_{5/2})^3$ with $\sim 15\%$; hence the calculated spectroscopic factor for single-nucleon transfer connecting the two states is quite small. This prediction is consistent with the experimental observations.

The next model state is 3^+ , coming at 0.9 MeV excitation. The largest components of its wave function resemble a $d_{5/2}$ neutron coupled to the main components of the ground state of ^{19}F , and hence a large $l=2$ spectroscopic factor is predicted for the $^{19}\text{F}(d, p)^{20}\text{F}$ transition to this level. The first experimentally observed excited state, the one at 0.655 MeV, has been assigned³⁻⁷ as either 1^+ or 3^+ , and the recent (d, p) polarization measurements of Quin and Vigdor¹⁷ definitely indicate 3^+ . The spectroscopic strength measured for this state is the largest measured for $l=2$ transfer. Hence, the model and the data agree on the most obvious characteristics of the first excited state.

There are two model states between 1- and 2-MeV excitation energy, one with $J^\pi = 1^+$ and one with 4^+ . The observation of a very weak $l=0$ transition to the 1.056-MeV experimental state is consistent with its 1^+ assignment. The strength of the transition and the energy of the state are consistent only with the characteristics of the first 1^+ state predicted by the model. There are three other experimental levels in the neighborhood of 1 MeV excitation. In all probability, one of them is the 4^+ state, since the predicted energies of high-spin states are, on all previous evidence, quite reliable.²³

The most likely candidate for the 4^+ state is the state at 0.823 MeV. Correlation studies^{7,13} appear not to discriminate between assignments of 2^+ and 4^+ . If correct, the $l=2$ assignment of El Bedewi⁴ in his 8.9-MeV study of the reaction $^{19}\text{F}(d, p)^{20}\text{F}$ would eliminate the 4^+ possibility. However, an $l=2$ assignment is not required in the present study. In fact, if $l=2$ is assumed and $(2J+1)S$ is extracted by consistent DWBA analyses of the 8.9- and 16-MeV $^{19}\text{F}(d, p)^{20}\text{F}$ data for this state, the value obtained at 8.9 MeV is 10 times that at 16 MeV. This result is rather strong evidence against the previous $l=2$ assignment, since

such an order-of-magnitude change in spectroscopic strength would be the signature of a non-direct mechanism (e.g., a two-step process). Moreover, since the earlier $l=2$ assignment was the only strong evidence for positive parity for this state, even the parity may now be open to question.

The measured mean lifetimes for the 0.823-MeV state^{13,14} lead to a weighted $\tau = 78 \pm 10$ psec. For $J=2$, the measured⁷ mixing ratio is $\delta = 2.1$ for the decay to the ground state. These two results lead to a very large $M1$ hindrance factor^{7,13} if the 0.823-MeV state has $J^\pi = 2^+$. Further evidence for a 4^+ assignment comes from the $T=1$ states in ^{20}Ne . The 10.27-MeV level of ^{20}Ne has been identified²⁹ as the analog of the ^{20}F ground state. A probable assignment²⁹ of $(4^+, T=1)$ to a state at 11.08 MeV in ^{20}Ne would require a 4^+ state near 0.8 MeV in ^{20}F . Finally, if the 1.824-MeV state (discussed below) has $J=5$, then $J=2$ can be ruled out for the 0.823-MeV state.

For the remaining two experimental levels in this region (those at 0.98 and 1.31 MeV), the dominant components in the wave functions could be configurations involving excitation of particles from the $1p$ shell into the sd shell. There is some evidence³⁰ that the 0.983-MeV state may have negative parity. More definitive evidence on the parities in this region would be very valuable.

Clustered about 2.2 MeV excitation in the $K+12$ FP model spectrum are states with $J^\pi = 2^+$, 5^+ , and 3^+ . A quintuplet of states occurs around 2 MeV in the experimental spectrum. The next states in both the model and experimental spectra occur at about 3 MeV. Hence, we suspect that two of the five experimental states near 2 MeV also have their origins outside the sd -shell space, although this conclusion is more closely tied to the present $K+12$ FP Hamiltonian form than is the previous discussion. The 2^+ state predicted by the model has a wave function similar to that of the first 3^+ , with the main components of the $\frac{1}{2}^+$ ground state of ^{19}F and with the $d_{5/2}$ neutron coupled to $J=2$ instead of $J=3$. The large $l=2$ spectroscopic factor measured for the experimental 2.044-MeV level indicates that it should be identified with this model 2^+ state. This result is consistent with the assignment of Ref. 7.

The weak observed $l=2$ transition to the experimental 2.196-MeV level, suggested to be 3^+ , is consistent with the second 3^+ state predicted by the model, but the association cannot be made as definitely as for the 2^+ . One of the remaining three experimental levels located around 2-MeV excitation energy should have $J^\pi = 5^+$, but as in the case of the 4^+ state, no assignment has yet been made. The γ decay of the 1.824-MeV state, to-

gether with its nonobservation in the present reaction, points to the 1.824-MeV state as the probable 5^+ state. It decays primarily^{3,4} to the 0.823-MeV state. If the 0.823-MeV state has $J=2$, then the J for the 1.824-MeV level is⁷ 1, 2, or 3, whereas if the 0.823-MeV state has $J=4$, the spin of the 1.824-MeV state is⁷ 3 or 5. However, if the reported⁷ weak γ -decay branch to the 2^+ ground state is confirmed, a 5^+ assignment is unlikely. The 1.971-MeV state may have negative parity.³⁰ An earlier assignment¹⁸ of $J^\pi=(3^-)$ to a state at 1.85 MeV is not definite, since that work did not resolve the 1.824-1.840-MeV doublet.³¹

Levels above 3 MeV excitation will be discussed only if they are predicted to have significant $l=0$ stripping strengths. The model calculation puts a 0^+ and a 1^+ level together at 3.3 MeV excitation. These states may be thought of as the $J=0$ and $J=1$ couplings of a $2s_{1/2}$ neutron to the $\frac{1}{2}^+$ ground state of ^{19}F . Two strong $l=0$ transitions are observed to levels at 3.5 MeV in the experimental spectrum. The present data, together with two-particle-transfer data,¹⁹ have led to an assignment of 1^+ for the 3.489-MeV state and 0^+ for the 3.531-MeV state. It is highly probable that these experimental levels correspond to the 1^+ and 0^+ model states. The experimental level at 4.09 MeV, which is observed to have an $l=0+2$ character, most likely corresponds to the 1^+ model state at 4.1 MeV. The 1^+ state predicted at 4.69 MeV may be the state observed at 4.32 MeV with a pure $l=0$ (d, p) angular distribution.

Those states with $J \leq 3$ below $E_x = 4.5$ MeV that have probable theoretical counterparts are listed in Table IV, where the experimental and theoret-

cal excitation energies and spectroscopic strengths are compared. (Except for the state at 3.686 MeV, these are the states whose angular distributions are shown in Fig. 2.) The agreement between experiment and theory appears to be quite good. The fact that the calculated spectroscopic factors are generally larger than the experimental ones may be due to an uncertainty in extraction of absolute spectroscopic factors and/or to the neglect of core excitation in the shell-model calculations.

V. CONCLUSION

A considerable portion of the low-energy level scheme of ^{20}F can be understood in terms of a shell model based upon a closed ^{16}O core. In particular, the pattern of spectroscopic strengths observed in the reaction $^{19}\text{F}(d, p)^{20}\text{F}$ is predicted quantitatively by the model. States with $J^\pi=3^+$ and 2^+ , formed by coupling a $1d_{5/2}$ neutron to the $\frac{1}{2}^+$ ground state of ^{19}F , are identified at 0.66 and 2.1 MeV, respectively. The 1^+ and 0^+ states formed by coupling a $2s_{1/2}$ neutron to the same core are located at 3.49 and 3.53 MeV, respectively.

Of the 11 states experimentally observed below 2.5 MeV, only 7 can be accounted for by the model. Two of these model states, the 4^+ and 5^+ , remain to be positively identified experimentally. The four extra experimental states presumably have their origin outside the basis space of the model, probably in excitations out of the ^{16}O core. Recent calculations³² have predicted four negative-parity states ($J^\pi=2^-, 1^-, 3^-,$ and 2^-) below 2.5 MeV in ^{20}F . The four states below 2.5 MeV not accounted for by the sd -shell model are those at 0.983, 1.309,

TABLE IV. Comparison of experimental and theoretical spectroscopic factors for $^{19}\text{F}(d, p)^{20}\text{F}$.

E_x (MeV)	Experimental values			E_x (MeV)	Theoretical values ^b		
	J^π	(2J+1)S			J^π	(2J+1)S	
		$l=0$	$l=2^a$			$l=0$	$l=2$
0	2^+		≤ 0.06	0	2^+		0.15
0.657	3^+		2.59	0.92	3^+		4.48
1.058	1^+	0.02	≤ 0.03	1.34	1^+	0.24	0.03
2.044	(2^+)		2.32	2.12	2^+		3.45
2.196	(3^+)		0.50	2.41	3^+		0.56
2.967	(3^+)		0.36	3.12	3^+		0.35
3.489	1^+	1.20		3.29	1^+	0.96	0.09
3.531	0^+	0.28		3.33	0^+	0.53	
(3.590)	(2^+), (1^+)	(≤ 0.09)	(0.42)	3.56	2^+		0.05
3.686	(3^+)		≤ 0.04	3.88	3^+		0.07
4.089	(1^+)	0.18	0.10	4.09	1^+	0.66	0.30
4.282	(2^+)		0.07	4.17	2^+		0.05
4.320	(0^+), (1^+)	0.27	—	4.69	1^+	0.18	0.27
Sum		2.05	6.43			2.57	9.85

^a Extracted on the assumption of $d_{3/2}$ for 1^+ states and $d_{5/2}$ for others.

^b Theoretical excitation energies and spectroscopic factors are the $K+12$ FP model results given in Ref. 23.

1.840, and 1.971 MeV. Proton pickup on ^{21}Ne should easily establish whether these are negative-parity states.

ACKNOWLEDGMENTS

The authors would like to thank Dr. Paul Quin for communicating his results prior to publica-

tion and for many extremely valuable discussions. We also acknowledge interesting discussions with D. Kurath, E. C. Halbert, J. B. McGrory, and J. D. Garrett. We thank Charles Bolduc and Miss Elizabeth Brennan for their help in various phases of data accumulation and analysis. The assistance of Jack Wallace and the tandem crew at Argonne is gratefully acknowledged.

† Work performed under the auspices of the U. S. Atomic Energy Commission.

* Present address: Physics Department, University of Pennsylvania, Philadelphia, Pennsylvania 19104.

‡ Present address: Physics Department, University of Kansas, Lawrence, Kansas 66044.

¹F. A. El Bedewi, Proc. Phys. Soc. (London) **A69**, 221 (1956).

²A. A. Rollefson, P. F. Jones, and R. J. Shea, Phys. Rev. C **1**, 1761 (1970).

³P. R. Chagnon, Nucl. Phys. **59**, 257 (1964).

⁴G. A. Bissinger, R. M. Mueller, P. A. Quin, and P. R. Chagnon, Nucl. Phys. **A90**, 1 (1967).

⁵P. A. Quin, Ph.D. thesis, University of Notre Dame, 1968 (unpublished).

⁶P. A. Quin, A. A. Rollefson, G. A. Bissinger, C. P. Browne, and P. R. Chagnon, Phys. Rev. **157**, 991 (1967).

⁷P. A. Quin, G. A. Bissinger, and P. R. Chagnon, Nucl. Phys. **A155**, 495 (1970).

⁸T. Holtebekk, S. Tryti, and G. Vamraak, Nucl. Phys. **A134**, 353 (1969).

⁹E. G. Nadjakov, Nucl. Phys. **48**, 492 (1963).

¹⁰I. Berquist, J. A. Biggerstaff, J. H. Gibbons, and W. M. Good, Phys. Rev. **158**, 1049 (1967).

¹¹H. Spilling, H. Gruppelaar, H. F. de Vries, and A. M. J. Spits, Nucl. Phys. **A113**, 395 (1968).

¹²R. Hardell and A. Hasselgren, Nucl. Phys. **A123**, 215 (1969).

¹³J. G. Pronko and R. W. Nightingale, Phys. Rev. C **4**, 1023 (1971).

¹⁴R. J. Nickles, Nucl. Phys. **A134**, 308 (1969).

¹⁵R. L. Hershberger, M. J. Wozniak, Jr., and D. J. Donahue, Phys. Rev. **186**, 1167 (1969).

¹⁶T. Holtebekk, R. Strømme, and S. Tryti, Nucl. Phys.

A142, 251 (1970).

¹⁷P. A. Quin and S. E. Vigdor, Bull. Am. Phys. Soc. **15**, 1686 (1970); and to be published.

¹⁸J. C. Hardy, H. Brunnader, and J. Cerny, Phys. Rev. Letters **22**, 1439 (1969).

¹⁹H. T. Fortune, J. D. Garrett, J. R. Powers, and R. Middleton, Phys. Rev. C **4**, 850 (1971).

²⁰F. Ajzenberg-Selove, to be published.

²¹E. Freiburg and V. Zörgel, Z. Physik **162**, 114 (1961).

²²G. Scharff-Goldhaber, A. Goodman, and M. G. Silbert, Phys. Rev. Letters **4**, 25 (1960).

²³E. C. Halbert, J. B. McGrory, B. H. Wildenthal, and S. P. Pandya, in *Advances in Nuclear Physics*, edited by M. Baranger and E. Vogt (Plenum, New York, 1971), Vol. 4.

²⁴R. H. Bassel, R. M. Drisko, G. R. Satchler, L. L. Lee, Jr., J. P. Schiffer, and B. Zeidman, Phys. Rev. **136**, B960 (1964).

²⁵P. D. Kunz, private communication. We are grateful to Professor Kunz for making the code DWUCK available to us.

²⁶See, for example, J. D. Garrett, R. Middleton, and H. T. Fortune, Phys. Rev. C **4**, 165 (1971).

²⁷B. A. Watson, P. P. Singh, and R. E. Segel, Phys. Rev. **181**, 977 (1969).

²⁸T. T. S. Kuo, Nucl. Phys. **A103**, 71 (1967).

²⁹J. D. Pearson and R. H. Spear, Nucl. Phys. **54**, 434 (1964).

³⁰H. T. Fortune, J. D. Garrett, and R. Middleton, to be published.

³¹J. C. Hardy, private communication.

³²I. P. Johnstone, B. Castel, and P. Sostegno, Phys. Letters **34B**, 34 (1971).